Single Transition State Serves Two Mechanisms. Ab Initio Classical Trajectory Calculations of the Substitution−Electron Transfer Branching Ratio in $CH_2O^{\bullet-} + CH_3Cl$

Jie Li,[†] Xiaosong Li,[†,‡] Sason Shaik,[§] and H. Bernhard Schlegel*[,†]

Department of Chemistry, Wayne State University, Detroit, Michigan 48202, Department of Organic Chemistry, Hebrew University, Jerusalem 91904, Israel, and the Lise Meitner-Minerva Center of Computational Chemistry, Hebrew University, Jerusalem 91904, Israel

Received: July 16, 2004

The reaction of a formaldehyde radical anion with methyl chloride is an example of a reaction in which a single transition state serves two mechanisms: substitution at carbon (Sub(C)) and electron transfer (ET). This reaction has been studied by ab initio molecular dynamics at the HF/6-31G(d) level of theory. Initial conditions were sampled from thermal distributions at the transition state, and ca. 200 trajectories were calculated at each of four different temperatures. Some trajectories go directly to ET products, but most go to the Sub(C) valley. Analysis of the initial conditions did not reveal any definitive factors that consistently favored one channel over the others. About half of the molecules in the Sub(C) valley subsequently dissociate to ET products within the 800−1200-fs simulation time of the present calculations. These molecules showed unimolecular kinetics for dissociation consistent with a chemically activated species. The ratio of ET to Sub(C) products varied from 1.02 to 1.43 over the temperature range 148−598 K. In a kinetic investigation of the reaction mechanism, such a temperature dependence would give the semblance of two competing transition states having different structures. However, since one transition state serves both mechanisms, the temperature dependence of the branching ratio is a reflection of the shape of the potential energy surface, and not an indicator of separate transition states.

Introduction

Physical organic chemistry has revealed intriguing phenomena where related mechanisms generate a reactivity spectrum with a borderline region in which the two mechanisms seem to merge and have transition states of hybrid characters.[1,2] The most celebrated examples are the S_N2-S_N1 spectrum and the β-elimination E2−E1 spectrum,[3−5] with their borderline regions, which possess properties of the two extreme mechanisms. Another well-known relationship is between substitution and electron-transfer reactions, which also exhibit borderline regions.[6−22] The borderline region is typified by entangled reactivity,[9] where commonly established experimental methods encounter difficulties in definitively assigning the reaction mechanisms. In some cases, the borderline region may involve similar reaction rates through two different transition states. However, a more interesting case occurs when two different products can be formed via the same transition state. Reactions between ketyl radical anions and alkyl halides are examples of this intriguing situation, in which both electron transfer (ET) products and substitution at carbon (Sub(C)) products can be formed via the same, tightly bound transition state.[23−33] Such cases are especially tantalizing since varying the temperature may well lead to different proportions of the products, thereby giving the semblance of competing mechanisms with two different transition states having distinct structural properties.

The ET/Sub(C) dichotomy in the $CH_2O^{\bullet-} + CH_3Cl$ reaction has been the subject of numerous theoretical studies.[25−33] The ET products can be formed either by an outersphere electron transfer reaction or an innersphere reaction. The latter transition state is lower in energy and is of primary interest in the current work, because it also leads to Sub(C) products. The nature of this transition state has been firmly established at a variety of levels of theory.[25−33] From this transition state, the potential energy surface descends monotonically toward product clusters. As it descends, the valley bifurcates, with one branch yielding Sub(C) products and the other leading to ET products. Since the bifurcation of the potential energy surface occurs after the transition state, reaction-path-following techniques and transition-state theory cannot answer crucial questions about the branching ratios. Molecular dynamics is essential to probe the details of this reaction.

In earlier work, we used both reaction path following and ab initio trajectory calculations to explore the potential energy surface for reactions of ketyl radical anions with alkyl halides.[28,30] For $CH_2O^{\bullet-} + CH_3Cl$, we found that an internal coordinate steepest descent path from the transition state leads to ET products, while a reaction path in mass-weighted coordinates (intrinsic reaction coordinate, IRC) proceeds to Sub(C) products.[28] From ab initio classical trajectory calculations on a series of reactions, $CH_2O^{\bullet-} + CH_3X$ (X = F, Cl, Br) and $NCCHO^{\bullet-} + CH_3Cl$, we found that stronger C−X bonds and weaker electron donors favor substitution reactions over electron transfer.[30]

Yamataka, Aida, and Dupuis[32,33] (YAD) have also used ab initio molecular dynamics to investigate various aspects of the $CH_2O^{\bullet-} + CH_3Cl$ reaction. In their initial study, they found two types of trajectories: simple ones that lead directly to Sub(C) and more complex ones that eventually dissociate to ET products. In subsequent work, they extended their calculations

* hbs@chem.wayne.edu.
[†] Wayne State University.
[‡] Current address: Department of Chemistry, Yale University, New Haven, Connecticut 06520.
[§] Hebrew University.

10.1021/jp046827n CCC: $27.50
Published on Web 09/08/2004

to examine the effects of solvent relaxation and temperature.[33] Higher temperatures increase the amount of ET product and stronger relaxation reduces the number of Sub(C) trajectories that dissociate to ET. In addition to the Sub(C) and Sub(C) → ET channels, they also observed a few trajectories that proceeded directly to ET products independent of solvent relaxation strength and temperature. In recent work,[34] YAD calculated a small number of trajectories for the $NCCHO^{\bullet-} + CH_3Cl$ and $NCCHO^{\bullet-} + (CH_3)_2CHCl$ reactions and also found that cyano substitution favored the substitution reaction and increased steric effects favored electron transfer.

In the present work, we have undertaken a more extensive investigation of the $CH_2O^{\bullet-} + CH_3Cl$ reaction at several temperatures to obtain a more detailed understanding of this phenomenon of entangled reaction mechanisms.[9] With a larger number of trajectories and proper sampling that includes zero-point energy, we are able to calculate the branching ratio as a function of temperature, to examine the kinetics of Sub(C) versus Sub(C) → ET in more detail, and to see whether individual reaction channels are favored by particular initial conditions.

Methods. Electronic structure and molecular dynamics calculations were performed with the development version of the Gaussian series of programs.[35] Molecular dynamics simulations were carried out using ab initio classical trajectory calculations on the Born−Oppenheimer surface.[36] In this approach, a converged electronic-structure calculation is carried out each time that information about the potential energy surface is needed for the integration of the classical equations of motion for the atoms in the molecule. Trajectories were integrated with our Hessian-based predictor-corrector algorithm[37] using the UHF/6-31G(d) level of theory. A predictor step is taken on a quadratic function obtained from the Hessian or second derivatives of the potential energy surface. A corrector step is then computed on a fifth-order polynomial fitted to the energies, gradients, and Hessians at the beginning and end points of the predictor step. The Hessians are computed analytically using electronic structure calculations and then updated for five steps using gradients from electronic structure calculations before being recomputed analytically.[38]

As in our previous work,[30] the trajectories were started at the transition state and initial conditions were chosen to correspond to a thermal distribution.[39] Motion along the transition vector was directed toward the products and was sampled from a thermal distribution. Rotational energies were sampled from a thermal distribution of a symmetric top. Quasiclassical normal-mode sampling was used for the vibrational energies and included zero-point energy plus thermal energy.[39,40] For each initial condition, the vibrational phases were chosen randomly, and the momentum and displacement were scaled so that the vibrational kinetic energy and the potential energy obtained from the ab initio surface summed to the desired total energy (if proper scaling could not be achieved because of the anharmonicity of the potential energy surface, the trajectory was discarded). The calculations of YAD also started from a thermal distribution at the transition state but did not include zero-point energy or vibrational displacement in the initial conditions.

Trajectories were integrated with a step size of 0.5 $amu^{1/2}$ bohr. The total energy was conserved to better than 10^{-5} hartree. Since spurious angular forces were removed by projection, angular momentum was conserved to 10^{-9} $\hbar$. At each temperature, ca. 200 trajectories were integrated for up to 800−1200 fs starting at the transition state and ending when the products were well separated.

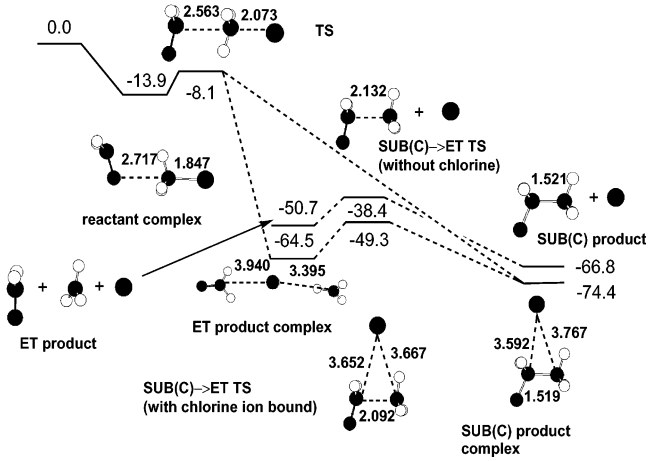

Figure 1. Energetics and optimized geometries of the transition states and products for the Sub(C)/ET reaction at the UHF/6-31G(d) level of theory.

SCHEME 1

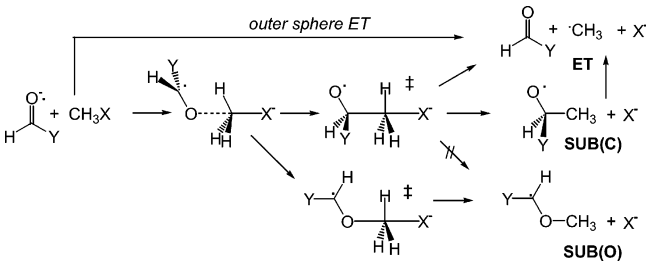

Results and Discussion

Structures and Energetics. The optimized geometries of the transition states and products are shown in Figure 1. As remarked previously,[25−33] the dependence of the geometry on the level of theory is relatively small. Reaction-path following has shown that the Sub(C)/ET transition state is connected to both the Sub(C) and ET channels.[28] The Sub(O) reaction proceeds through a different transition state that can be reached by going from the Sub(C)/ET transition state back to the reactant complex and then to the Sub(O) transition state (see Scheme 1). Formation of the ET products can occur directly or by dissociation of Sub(C) products.

At the UHF/6-31G(d) level of theory, the energies released on going from the transition state to the Sub(C) and ET products complexed with chloride ion are 66.3 and 56.4 kcal/mol, respectively, and are in good agreement with the calculations of YAD (65.2 and 50.8 kcal/mol at UHF/6-31+G(d)). For all of the trajectories calculated here, the chloride ion was well separated from the remaining products by the end of the trajectory. The corresponding energy releases without the chloride ion bound are 58.7 and 42.6 kcal/mol for Sub(C) and ET, respectively. The structures of the Sub(C) → ET transition states are similar with and without the chlorine ion bound, and are 25.1 and 28.4 kcal/mol above the corresponding Sub(C) structures. This is also in good agreement with the UHF/6-31+G(d) calculations of YAD (27.2 kcal/ mol when complexed with chloride). Higher levels of theory and inclusion of solvent effects will change the energetics and affect the branching ratios obtained from the dynamics.

Dynamics. The trajectories can be grouped into four categories. Even though the initial velocity along the transition vector is directed toward products, some trajectories return to reactants (no reaction, NR). A few trajectories go directly to the electron-transfer products (direct ET) with only a single recoil between

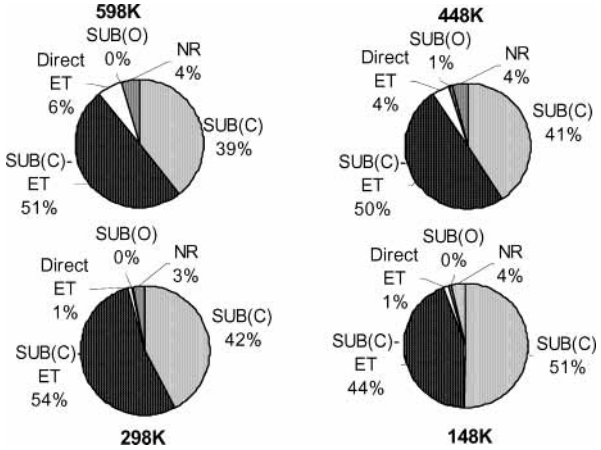

Figure 2. Branching ratios as a function of temperature.

TABLE 1: Number of Sub(C) and Sub(C) → ET, Direct ET, Sub(O), and NR Trajectories as a Function of Temperature

	temperature			
channel	148 K	298 K	448 K	598 K
sub(C)	102	86	83	80
sub(C) → ET	89	108	101	101
direct ET	3	2	9	13
sub(O)	1	1	2	0
NR	8	6	8	9

reactants, or equivalently, only one inner turning point for the C−C stretching motion. The majority of the trajectories proceed to the Sub(C) channel. Of these, a large fraction dissociate to ET products after more than one recoil or inner turning point in the C−C stretching motion (Sub(C) → ET). A very small number of trajectories end up as Sub(O) products, but do so via the reactant complex and the Sub(O) transition state.

The branching ratio for the Sub(C)/ET reaction is shown in Table 1 and Figure 2 for a number of temperatures. A rather wide temperature range (148−598 K) was chosen so that the trends can be seen more readily. At all temperatures, most of the trajectories start in the direction of substitution at carbon (Sub(C) plus Sub(C) → ET) and only a few go directly to ET products. This is in keeping with the intrinsic reaction coordinate (mass-weighted steepest descent path) that leads from the transition state to the Sub(C) products at this level of theory. YAD found qualitatively similar results. There is sufficient energy released as the molecule descends from the transition state, ca. 60 kcal/mol at UHF/6-31G(d), that it can readily go over the ridge that separates the ET products from Sub(C), a barrier of less than 30 kcal/mol. As the temperature increases, more energy is available and there is a small increase in the ratio of ET products, both in the direct channel and in the Sub(C) → ET channel. YAD also observed an increase in the direct channel, but did not report any branching ratios as a function of temperature. A major difference between the two studies is the fraction of the Sub(C) trajectories that subsequently dissociate to ET products. We find that about half of the trajectories that start in the Sub(C) direction dissociate to ET products, compared to ca. 15% in the trajectories calculated by YAD without solvent relaxation effects. As discussed above, the potential energy surfaces used in the two studies are very similar (in particular, the structures of the transition states, the energy differences between the transition state and the product complexes, and the barrier from Sub(C) to ET). One of the main differences between the two studies is the initial condition for vibration. In the present work, a physically realistic ensemble of starting structures and momenta is generated using quasiclassical normal-mode sampling, including zero-point energy as well as thermal energy, and by sampling initial displacements as well as momenta for the vibrational modes at the transition state. Thus, a larger and more appropriate region of the potential energy surface around the transition state is sampled by the present initial conditions. This feature and the fact that the trajectories are followed for a longer time could readily account for the larger fraction of Sub(C) → ET trajectories seen in the current study.

A variation of the branching ratio with temperature is often taken as evidence that the products are produced via distinct transition states.[12,17,18] Unless related by symmetry, these

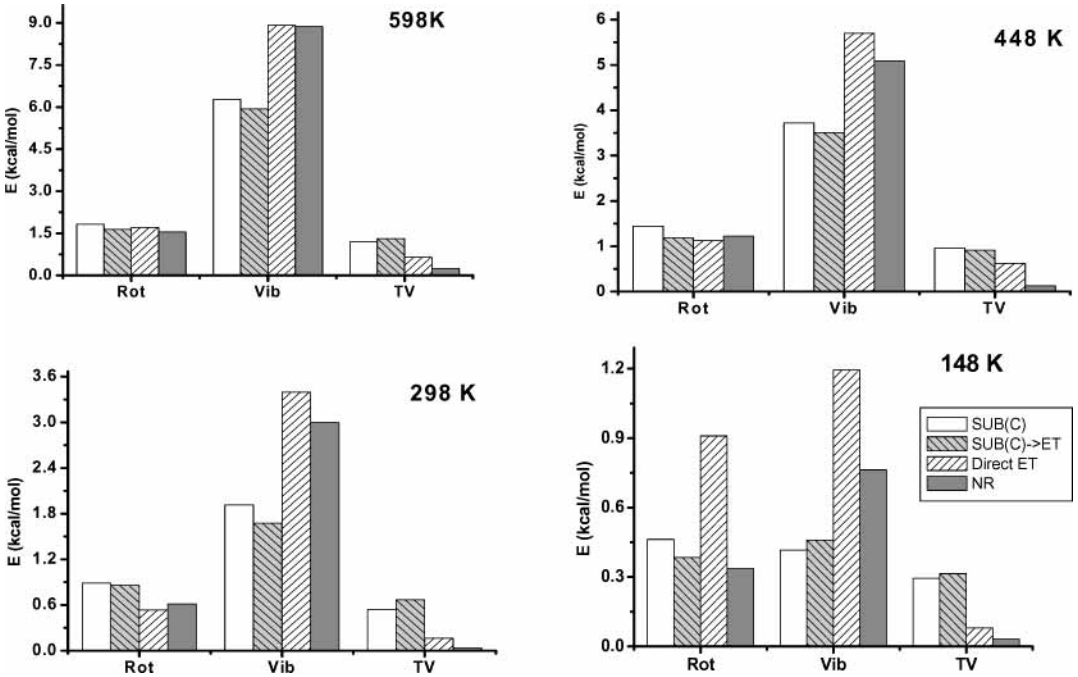

Figure 3. Average initial rotational energy (Rot), vibrational energy (Vib), and kinetic energy in the transition vector (TV) for the Sub(C), Sub(C) → ET, direct ET, and NR channels.

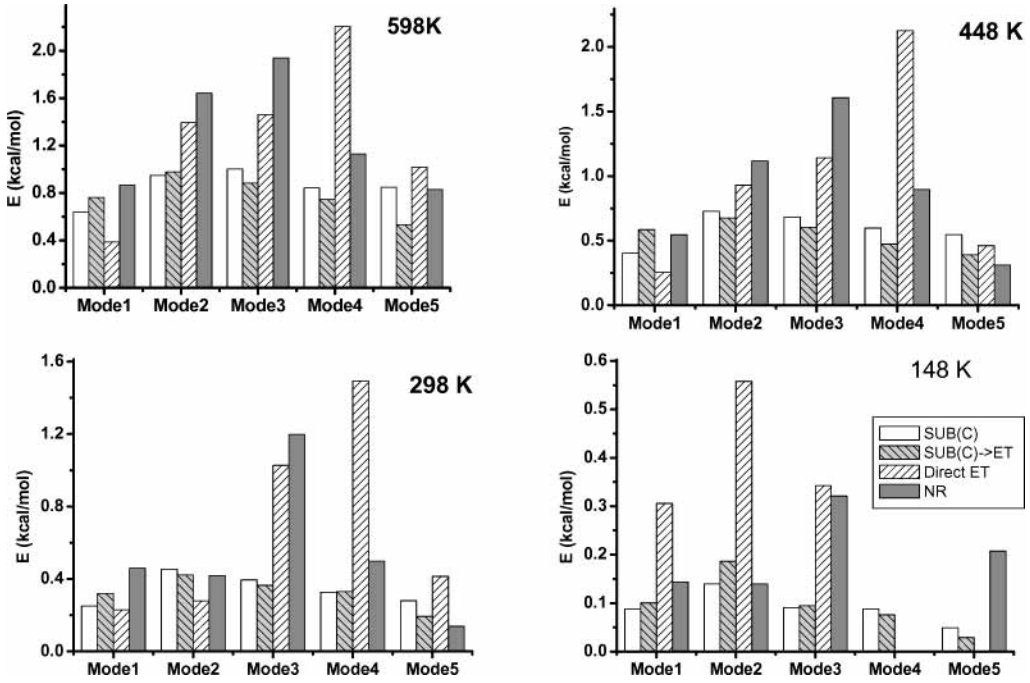

Figure 4. Average initial energy in the first five vibrational modes for the Sub(C), Sub(C) → ET, direct ET, and NR channels.

separate transition states would normally have different enthalpies of activation and also different entropies of activation. Hence, the ratio of the rates through these transition states will change with temperature. The present reaction is an obvious counterexample, since both products are formed via the same transition state. In this case, the modest temperature dependence arises from the topology of the potential energy surface. At low temperatures, there is little excitation of the vibrations perpendicular to the transition vector and, like the intrinsic reaction coordinate, the dynamics head into the Sub(C) valley. At higher temperatures, there is more vibrational energy available and the trajectories can explore a wider region of the potential energy surface, resulting in more ET products, both directly and via Sub(C) → ET.

Since all of the molecules at the transition state have enough energy to go to either Sub(C) or ET products, it would be desirable to understand what factors influence the ultimate fate of a molecule passing through the transition state. Figure 3 shows the initial energy distribution for the trajectories leading to Sub(C) and Sub(C) → ET, as well as direct ET and NR (there are too few Sub(O) trajectories to analyze). Any reliable trends should be discernible over the range of temperatures. The NR trajectories generally have less translational energy in the transition vector than direct ET. Although the direct ET trajectories dissociate after only one recoil, it is not because there is a greater amount of energy initially in the transition vector. The Sub(C) and Sub(C) → ET trajectories have more energy in the transition vector than direct ET, but survive one or more vibrations of the C−C bond. The average translation, rotation, and total vibrational energies are very similar for Sub(C) and Sub(C) → ET.

An examination of the initial energy in the individual vibrational modes, Figure 4, reveals a few features. At higher temperatures, the direct ET trajectories on average have somewhat more energy in mode 4 (C−C−Cl bend), whereas those that return to reactants (NR) have a bit more energy in modes 2 and 3 (bend and twist of CH_2O relative to CH_3Cl). However, there does not appear to be any statistically significant feature that distinguishes the Sub(C) and Sub(C) → ET channels. The distributions of the starting conditions (both displacement and velocities in each vibrational mode) for these two channels are broad and strongly overlapping. No one mode or simple combination of modes consistently leads to Sub(C) or consistently to Sub(C) → ET.

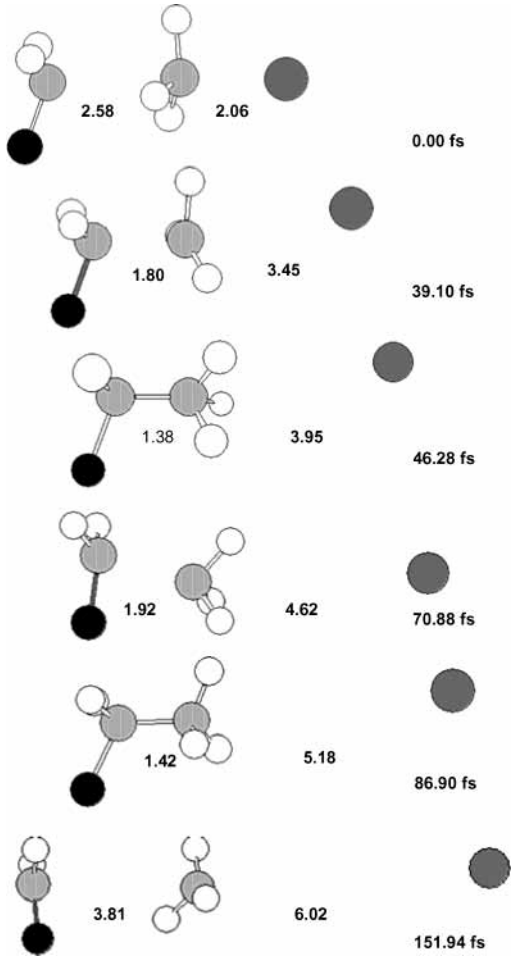

Figure 5. Snapshots of a typical Sub(C) → ET trajectory showing the transition state (0 fs) and two C−C inner turning points (46 and 87 fs) in the Sub(C) region, before dissociation into ET products.

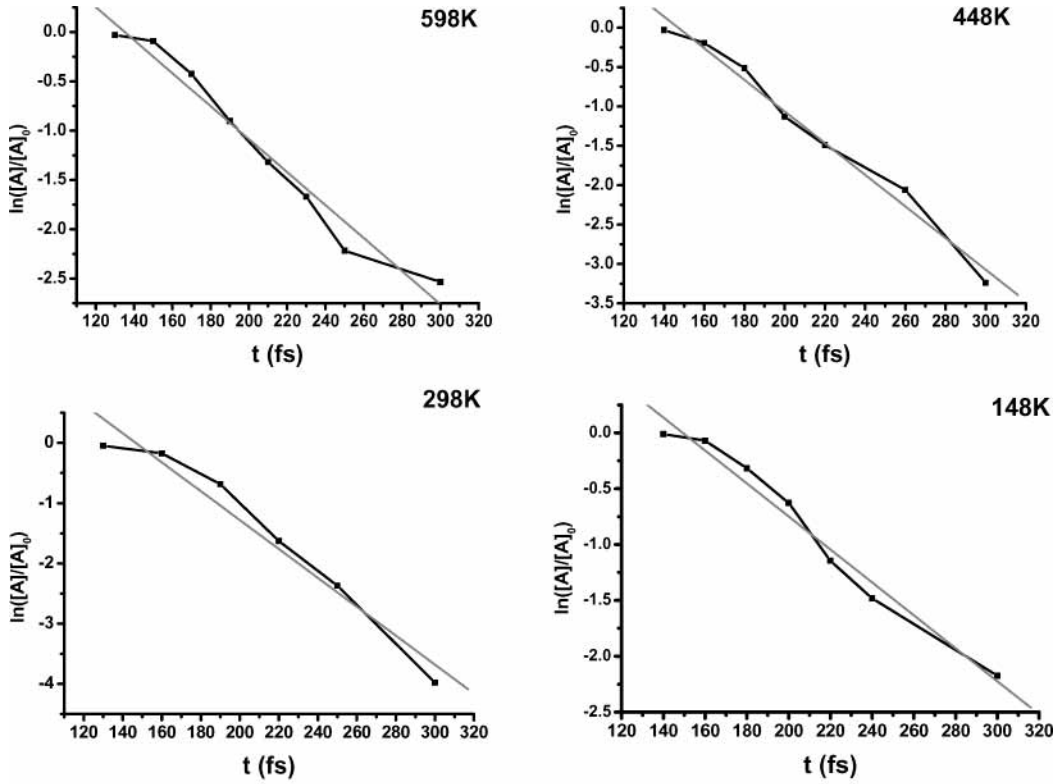

Figure 6. Plots showing first-order kinetics for Sub(C) → ET dissociation at $T = 148$, 298, 448, and 598 K.

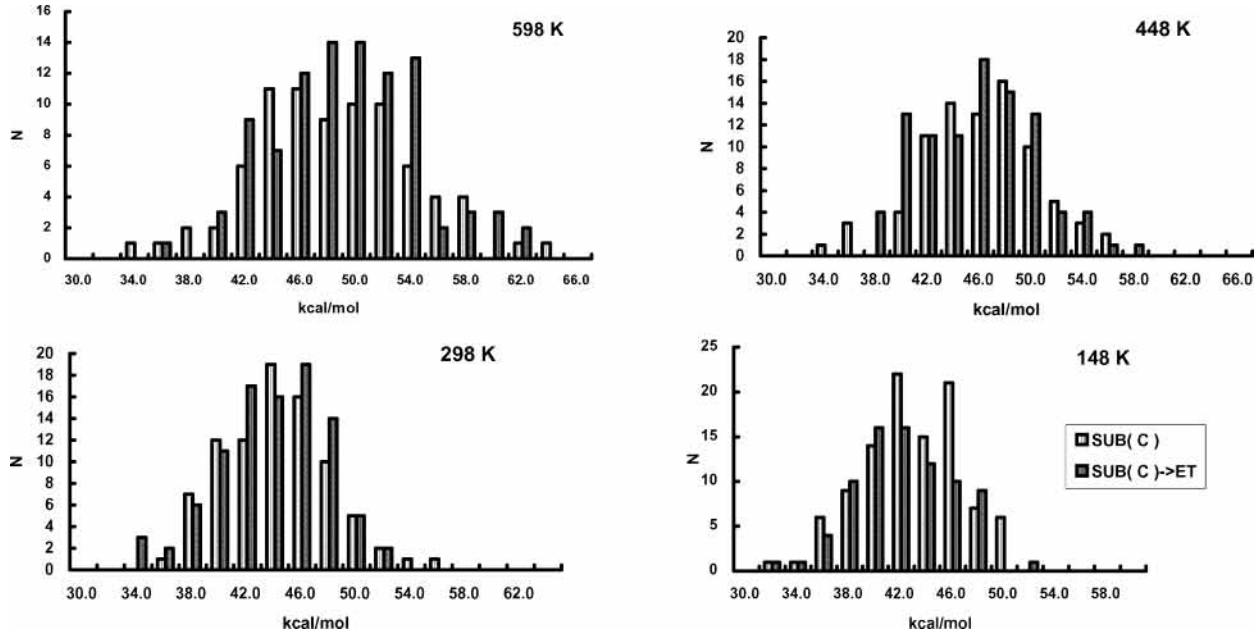

Figure 7. Final vibrational energies of $CH_3CH_2O^{\bullet}$ moiety in the Sub(C) and Sub(C) → ET trajectories.

Animation of the trajectories shows that most of the energy released is initially in the C−C stretching motion. As illustrated in Figure 5, a typical trajectory proceeds by shortening of the C−C bond. The distance of closest approach of the two carbons (i.e., the C−C bond length at the inner turning point) is ca. 1.4 Å for the Sub(C) and Sub(C) → ET trajectories. The H_2CO and CH_3 fragments then recoil[25−30] and the C−C distance increases. In the meantime, the Cl^- drifts away (slowly, because of its higher mass). Depending on the distribution of the energy, there can be one or more oscillations of the C−C bond. If the C−C bond remains intact, the trajectory yields Sub(C) products. On the other hand, a large number of the trajectories dissociate after a few C−C oscillations, leading to the Sub(C) → ET channel. For direct ET trajectories, the closest approach of the fragments is approximately 2 Å; the fragments recoil and separate to ET products usually in less than 100 fs.

Analysis of the Sub(C) → ET trajectories shows that about half of them have dissociated to ET products in 180−200 fs. The lifetimes are longer for lower temperatures, as might be anticipated for processes with a substantial barrier. By 150 fs,

the Cl^- is on average 4.0 Å from the rest of the molecule. This suggests that the Sub(C) → ET trajectories are characterized by the unimolecular dissociation of the $CH_3CH_2O^\bullet$ fragment in the Sub(C) product valley. Figure 6 plots the logarithm of the number of undissociated $CH_3CH_2O^\bullet$ molecules in the Sub(C) → ET channel as a function of time. As expected for a first-order reaction, the unimolecular dissociation yields a linear plot. However, the rate constants for Sub(C) → ET derived from these plots (0.015 ± 0.001, 0.018 ± 0.001, 0.020 ± 0.001, and 0.017 ± 0.001 fs^{-1} for 148−598 K) do not vary significantly with temperature, contrary to what would be expected from thermal rate constants for a process with a barrier of 25−30 kcal/mol. This indicates that the available energy is not in thermal equilibrium distribution throughout the molecule. Rather, this indicates that the reaction occurs via a chemically activated process in which the energy is stored in a few vibrational modes. In particular, the energy deposited in the C−C bond during the initial displacement reaction does not have sufficient time to equilibrate with the remaining vibrational modes before the molecule dissociates.

The $CH_3CH_2O^\bullet$ fragment in the Sub(C) valley is produced with considerable internal energy. In keeping with a chemically activated process, the total vibrational energy for $CH_3CH_2O^\bullet$ has a peaked distribution, as shown in Figure 7, rather than a Boltzmann distribution. The vibrational energy distributions for the Sub(C) and Sub(C) → ET channels are strongly overlapping, and the average vibrational energies do not differ significantly. Thus, it is not the total vibrational energy but the distribution and relative phases that determine whether the CH_3CH_2O fragment dissociates rapidly (Sub(C) → ET) or remains bound (Sub(C)) during the 800−1200-fs simulation time. Since the ET production is driven by energy localized in or near the C−C bond, the dissipation of the excess energy to the environment (solvent) will reduce the yield of ET product. YAD found that a reasonable value for the solvent relaxation parameter ($\tau \sim$ 2000 fs) reduced the amount of Sub(C) → ET product by ca. 20%, but did not turn off this channel. This suggests that this mechanism, and hence the entangled reactivity, will persist in solution. However, the branching ratios may be quite different in solution, since interaction with the solvent could change the energetics of the reaction significantly.

Summary

Classical trajectory calculations have been used to study the reaction of formaldehyde radical anion with methyl chloride. In this novel reaction, one transition state leads to two different products. Both channels are energetically accessible and the ratio of ET to Sub(C) products varies from 1.02 to 1.43 over a temperature range of 148 K to 598 K. Although some trajectories go directly to ET products, most go to the Sub(C) valley. A large fraction of these molecules subsequently dissociate to ET products. Thus, the Sub(C) → ET pathway is the dominant source of ET products in the gas phase. Molecular dynamics calculations show that the Sub(C)/ET ratio varies with temperature. The present calculations demonstrate that for this reaction the variation in the branching ratio with temperature is due to the topology of the potential energy surface after a single transition state. It is not the result of the reaction proceeding via two different transition states. This type of entangled reactivity may be wide-ranging and applicable to other borderline situations, such as S_N2-S_N1, E2−E1, etc. There is a challenge here for both theory and experiment to devise probes that can distinguish "normal" situations, with two transition states for two mechanisms, from entangled situations with one transition state for two mechanisms.

Acknowledgment. This work was supported by a grant from the National Science Foundation (CHE 0131157). The authors thank C&IT and ISC at Wayne State University and NCSA for computer time.

References and Notes

(1) Lowry, T. H.; Richardson, K. S. *Mechanism and Theory in Organic Chemistry*, 3rd ed.; Harper & Row: New York, 1987.

(2) Ingold, C. *Structure and Mechanism in Organic Chemistry*, 2d ed.; Cornell University Press: Ithaca, 1969.

(3) Saunders: W. H. Distinguishing between concerted and nonconcerted eliminations. *Acc. Chem. Res.* **1976**, *9*, 19−25.

(4) Jencks, W. P. When is an intermediate not an intermediate? Enforced mechanisms of general acid−base, catalyzed, carbocation, carbanion, and ligand exchange reaction. *Acc. Chem. Res.* **1980**, *13*, 161−169.

(5) Knier, B. L.; Jencks, W. P. Mechanism of reactions of N−(methoxymethyl)-N,N-dimethylanilinium ions with nucleophilic reagents. *J. Am. Chem. Soc.* **1980**, *102*, 6789−6798.

(6) Bank, S.; Noyd, D. A. Evidence for an Electron-Transfer Component in a Typical Nucleophilic Displacement Reaction. *J. Am. Chem. Soc.* **1973**, *95*, 8203−8205.

(7) Pross, A. The single electron shift as a fundamental process in organic chemistry: the relationship between polar and electron-transfer pathways. *Acc. Chem. Res.* **1985**, *18*, 212−219.

(8) Shaik, S. The Collage of S_N2 Reactivity Patterns: A State Correlation Diagram Model. *Prog. Phys. Org. Chem.* **1985**, *15*, 195−338.

(9) Shaik, S.; Shurki, A. Valence Bond Diagrams and Chemical Reactivity. *Angew. Chem., Int. Ed. Engl.* **1999**, *38*, 586−625.

(10) Daasbjerg, K.; Christensen, T. B. Investigation of the Competition between Electron-Transfer and S(N)2 in the Reaction between Anthracene Radical-Anion and the Methyl Halides. *Acta Chem. Scand.* **1995**, *49*, 128−132.

(11) Daasbjerg, K.; Pedersen, S. U.; Lund, H. On the Occurrence of Electron-Transfer in Aliphatic Nucleophilic-Substitution. *Acta Chem. Scand.* **1991**, *45*, 424−430.

(12) Lund, H.; Daasbjerg, K.; Lund, T.; Pedersen, S. U. On Electron-Transfer in Aliphatic Nucleophilic-Substitution. *Acc. Chem. Res.* **1995**, *28*, 313−319.

(13) Eberson, L. Application of the Dewar−Zimmermann Rules to the Reaction between Radical Cations and Nucleophiles. *J. Chem. Soc., Chem. Commun.* **1975**, 826−827.

(14) Lexa, D.; Saveant, J. M.; Su, K. B.; Wang, D. L. Single Electron-Transfer and Nucleophilic-Substitution − Reaction of Alkyl Bromides with Aromatic Anion Radicals and Low Oxidation-State Iron Porphyrins. *J. Am. Chem. Soc.* **1988**, *110*, 7617−7625.

(15) Cho, J. K.; Shaik, S. Electron-Transfer Vs Polar Mechanisms − Transition-State Structures and Properties for Reactions of a Cation Radical and a Nucleophile. *J. Am. Chem. Soc.* **1991**, *113*, 9890−9891.

(16) Hebert, E.; Mazaleyrat, J. P.; Welvart, Z.; Nadjo, L.; Saveant, J. M. Aromatic Anion Radicals and Dianions − Redox Reagents and or Nucleophiles − Partial Inversion of Configuration in the Electrochemical and Chemical Reductive Alkylation of Anthracene. *Nouv. J. Chim.* **1985**, *9*, 75−81.

(17) Daasbjerg, K.; Hansen, J. N.; Lund, H. On the Coupling of Anion Radicals with Sterically Hindered Alkyl-Halides. *Acta Chem. Scand.* **1990**, *44*, 711−714.

(18) Saveant, J. M. Dissociative Electron-Transfer − New Tests of the Theory in the Electrochemical and Homogeneous Reduction of Alkyl-Halides. *J. Am. Chem. Soc.* **1992**, *114*, 10595−10602.

(19) Lund, T.; Lund, H. Single Electron-Transfer as Rate-Determining Step in an Aliphatic Nucleophilic-Substitution. *Acta Chem. Scand. B* **1986**, *40*, 470−485.

(20) Lund, T.; Lund, H. Experimental Evaluation of the VBCM Model for Nucleophilic Substitutions. *Acta Chem. Scand. B* **1988**, *42*, 269−279.

(21) Speiser, B. Electron transfer and chemical reactions − Stepwise or concerted? On the competition between nucleophilic substitution and electron transfer. *Angew. Chem., Int. Ed. Engl.* **1996**, *35*, 2471−2474.

(22) Zipse, H. Electron-transfer transition states: Bound or unbound − That is the question! *Angew. Chem., Int. Ed. Engl.* **1997**, *36*, 1697−1700.

(23) Kimura, N.; Takamuku, S. Intramolecular Electron-Transfer and Sn2 Reactions in the Radical-Anions of 1-Benzoyl-Omega-Haloalkane Studied by Pulse- Radiolysis. *Bull. Chem. Soc. Jpn.* **1991**, *64*, 2433−2437.

(24) Kimura, N.; Takamuku, S. Mechanistic Evaluation of Dissociative Electron-Transfer and Nucleophilic-Substitution Reactions. *J. Am. Chem. Soc.* **1994**, *116*, 4087−4088.

(25) Sastry, G. N.; Shaik, S. Stereochemistry and Regiochemistry in Model Electron-Transfer and Substitution-Reactions of a Radical-Anion with an Alkyl Halide. *J. Am. Chem. Soc.* **1995**, *117*, 3290−3291.

(26) Sastry, G. N.; Shaik, S. Structured electron-transfer transition state. Valence bond configuration mixing analysis and ab initio calculations of the reactions of formaldehyde radical anion with methyl chloride. *J. Phys. Chem.* **1996**, *100*, 12241−12252.

(27) Sastry, G. N.; Danovich, D.; Shaik, S. Towards the definition of the maximum allowable tightness of an electron-transfer transition state in the reactions of radical anions and alkyl halides. *Angew. Chem., Int. Ed. Engl.* **1996**, *35*, 1098−1100.

(28) Shaik, S.; Danovich, D.; Sastry, G. N.; Ayala, P. Y.; Schlegel, H. B. Dissociative electron transfer, substitution, and borderline mechanisms in reactions of ketyl radical anions. Differences and difficulties in their reaction paths. *J. Am. Chem. Soc.* **1997**, *119*, 9237−9245.

(29) Sastry, G. N.; Shaik, S. Mechanistic crossover induced by steric hindrance: A theoretical study of electron transfer and substitution mechanisms of cyanoformaldehyde anion radical and alkyl halides. *J. Am. Chem. Soc.* **1998**, *120*, 2131−2145.

(30) Bakken, V.; Danovich, D.; Shaik, S.; Schlegel, H. B. A single transition state serves two mechanisms: An ab initio classical trajectory study of the electron transfer and substitution mechanisms in reactions of ketyl radical anions with alkyl halides. *J. Am. Chem. Soc.* **2001**, *123*, 130−134.

(31) Bertran, J.; Gallardo, I.; Moreno, M.; Saveant, J. M. Are anion radicals nucleophiles and/or outersphere electron donors? An ab initio study of the reaction of ethylene and formaldehyde anion radicals with methyl fluoride and chloride. *J. Am. Chem. Soc.* **1996**, *118*, 5737−5744.

(32) Yamataka, H.; Aida, M.; Dupuis, M. One transition state leading to two product states: ab initio molecular dynamics simulations of the reaction of formaldehyde radical anion and methyl chloride. *Chem. Phys. Lett.* **1999**, *300*, 583−587.

(33) Yamataka, H.; Aida, M.; Dupuis, M. Analysis of borderline substitution/electron-transfer pathways from direct ab initio MD simulations. *Chem. Phys. Lett.* **2002**, *353*, 310−316.

(34) Yamataka, H.; Aida, M.; Dupuis, M. Ab initio molecular dynamics studies on substitution vs electron-transfer reactions of substituted ketyl radical anions with chloroalkanes: how do the two products form in a borderline mechanism? *J. Phys. Org. Chem.* **2003**, *16*, 475−483.

(35) Frisch, M. J.; Trucks, G. W.; Schlegel, H. B.; Scuseria, G. E.; Robb, M. A.; Cheeseman, J. R.; Montgomery, J. A.; Vreven, T.; Kudin, K. N.; Burant, J. C.; Millam, J. M.; Iyengar, S.; Tomasi, J.; Barone, V.; Mennucci, B.; Cossi, M.; Scalmani, G.; Rega, N.; Petersson, G. A.; Ehara, M.; Toyota, K.; Hada, M.; Fukuda, R.; Hasegawa, J.; Ishida, M.; Nakajima, T.; Kitao, O.; Nakai, H.; Honda, Y.; Nakatsuji, H.; Li, X.; Knox, J. E.; Hratchian, H. P.; Cross, J. B.; Adamo, C.; Jaramillo, J.; Cammi, R.; Pomelli, C.; Gomperts, R.; Stratmann, R. E.; Ochterski, J.; Ayala, P. Y.; Morokuma, K.; Salvador, P.; Dannenberg, J. J.; Zakrzewski, V. G.; Dapprich, S.; Daniels, A. D.; Strain, M. C.; Farkas, Ö.; Malick, D. K.; Rabuck, A. D.; Raghavachari, K.; Foresman, J. B.; Ortiz, J. V.; Cui, Q.; Baboul, A. G.; Clifford, S.; Cioslowski, J.; Stefanov, B. B.; Liu, G.; Liashenko, A.; Piskorz, P.; Komaromi, I.; Martin, R. L.; Fox, D. J.; Keith, T.; Al-Laham, M. A.; Peng, C. Y.; Nanayakkara, A.; Challacombe, M.; Gill, P. M. W.; Johnson, B.; Chen, W.; Wong, M. W.; Andres, J. L.; Gonzalez, C.; Head-Gordon, M.; Replogle, E. S.; Pople, J. A.; *Gaussian*, Revision B.02 ed.; Gaussian, Inc.: Pittsburgh, PA, 2002.

(36) Bolton, K.; Hase, W. L.; Peslherbe, G. H. Direct Dynamics of Reactive Systems. In *Modern Methods for Multidimensional Dynamics Computation in Chemistry*; Thompson, D. L., Ed.; World Scientific: Singapore, 1998; pp 143−189.

(37) Millam, J. M.; Bakken, V.; Chen, W.; Hase, W. L.; Schlegel, H. B. Ab Initio classical trajectories on the Born−Oppenheimer surface: Hessian-based integrators using fifth-order polynomial and rational function fits. *J. Chem. Phys.* **1999**, *111*, 3800−3805.

(38) Bakken, V.; Millam, J. M.; Schlegel, H. B. Ab Initio classical trajectories on the Born−Oppenheimer surface: Updating methods for Hessian-based integrators. *J. Chem. Phys.* **1999**, *111*, 8773−8777.

(39) Hase, W. L. Classical Trajectory Simulations: Initial Conditions. In *Encyclopedia of Computational Chemistry*; Schleyer, P. v. R., Allinger, N. L., Clark, T., Gasteiger, J., Kollman, P. A., Schaefer, H. F., III, Schreiner, P. R., Eds.; Wiley: Chichester, 1998; pp 402−407.

(40) Peslherbe, G. H.; Wang, H. B.; Hase, W. L. Monte Carlo Sampling for Classical Trajectory Simulations. *Adv. Chem. Phys.* **1999**, *105*, pp 171−201.